

The minor axis outflow of NGC 2146

A. Greve¹, N. Neininger², A. Tarchi², and A. Sievers³

¹ Institut de Radio Astronomie Millimétrique, 300 rue de la Piscine, 38406 St. Martin d'Hères, France

² Astronomisches Institut der Universität Bonn, 71 Auf dem Hügel, 53121 Bonn, Germany

³ Instituto Radioastronomía Milimétrica, Nucleo Central, 7 Avenida Divina Pastora, 18012 Granada, Spain

received date; accepted date

Abstract. X-ray and optical observations have shown that the supernova explosions and stellar winds of the starburst in NGC 2146 produce an outflow of hot material along the minor axis. This outflow is expected to have a more or less conical shape, on either side of the galactic plane, and cone walls of cooler material where the outflow is in shock contact with halo gas. We attempt to determine the geometry (diameter at the base and opening angle) and the physical parameters (velocity and density) of the material in the cone walls from the optical emission line and radio observations presented here, and from published X-ray, radio, and optical observations. We compare the outflow of NGC 2146 with the outflow of M 82.

Key words: galaxies: structure – galaxies: individual (NGC 2146) – galaxies: ISM

1. Introduction

In analogy to other starburst galaxies (Heckman et al. 1990, Lehnert & Heckman 1996 a), the supernova explosions and stellar winds of the strong star formation activity in NGC 2146 produce an outflow of hot gas along the minor axis. The outflow is collimated in the disk by a ring of dense molecular gas confining the star formation region, and hence appears at X-ray and optical wavelengths under ideal conditions as cones on either side of the galactic plane. Such an outflow is especially prominent in galaxies viewed edge-on, as in the case of M 82. The hot gas at a temperature of $10^7 - 10^8$ K, seen at X-rays, is confined to the inner part of the cones; the gas in the cone walls in shock contact with the halo material is at a temperature of $\sim 10^4$ K and emits the [forbidden] recombination lines of H_α , [NII], [SII], etc. The outflowing hot gas may drag cool gas and dust out of the disk at the inner edge of the molecular ring and transports this material, and angular momentum, to a considerable height in the halo. The structure of such an outflow is schematically shown by Heckman et al. (1990, their Fig. 1) and clearly seen in

M 82 at X-ray (Schaaf et al. 1989, Bregman et al. 1995) and optical wavelengths (Axon & Taylor 1978, Bland & Tully 1988, Shopbell & Bland-Hawthorn 1998, McKeith et al. 1995, Devine & Bally 1999). Predictions, calculations, and interpretations of these outflows under the aspect of energy input, outflow velocity, density and temperature of the gas, and height of the outflow were published by Chevalier & Clegg (1985), Tomisaka & Ikeuchi (1988), Umemura et al. (1988), Yokoo et al. (1993), and others.

The X-ray and optical emission of the outflow in NGC 2146 was observed by Armus et al. (1995) and Della Ceca et al. (1999). Ultra-compact/ultra-dense H II regions containing many O-type stars, and radio supernovae and supernova remnants were recently detected in the starburst region in a combination of MERLIN and VLA observations by Tarchi et al. (2000).

Optical spectroscopy observations with the slit oriented along the minor axis show under favourable geometrical conditions characteristic velocity-split emission lines (M 82); conversely, measurement of the line splitting allows a determination of the outflow geometry and the outflow velocity. Unfortunately, for reasons to be explained below, in NGC 2146 there is no very clear detection of line splitting and hence the geometry and the velocity of the outflow is not well known, although the galaxy is seen tilted from edge-on by only $25 - 30^\circ$. From a combination of the observations of this paper (optical spectroscopy, CO line interferometer data) and published X-ray, radio, and optical measurements we attempt to determine the geometry and the physical parameters of the outflow cones: i.e. the diameter (b) of the base in the galactic plane, the opening angle (Θ), the outflow velocity (V), and the (electron) density (n_e) of the material in the cone walls. We compare the outflow of NGC 2146 with the well studied outflow of M 82.

2. The starburst galaxy NGC 2146

NGC 2146, at a distance of 14.5 Mpc (Benvenuti et al. 1975, for $H_0 = 75$; $1''$ is equivalent to 70 pc), is experiencing a starburst in the central region of ~ 2.5 kpc diameter. The molecular gas (CO) in this region is concen-

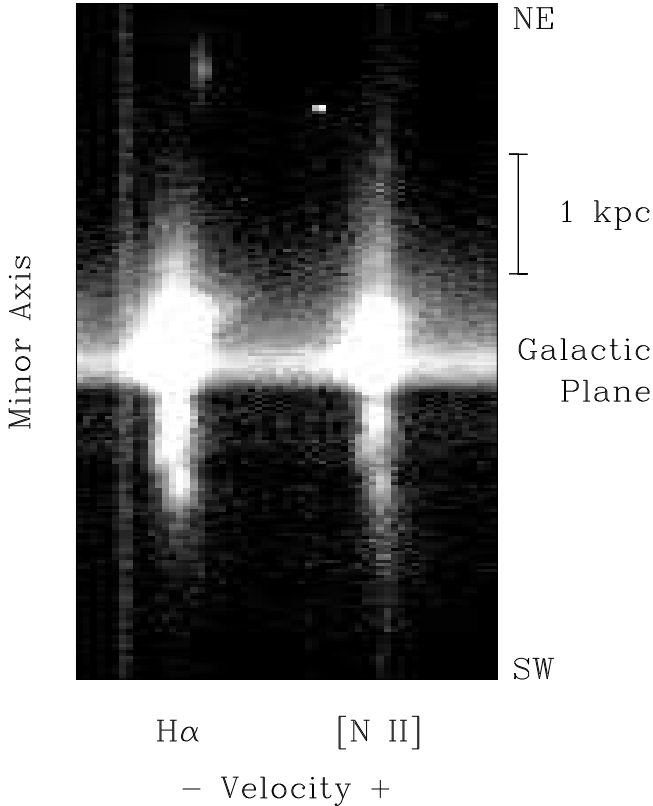


Fig. 1. $H\alpha$ 6563 Å and [NII] 6583 Å measured along the minor axis ($pa = 50^\circ$) of NGC 2146. The [vertical] straight line at the very left is a sky emission line. The [horizontal] continuum emission comes from a region near the center of the galactic plane. Note the increased emission from an H II region complex at ~ 2.5 kpc NE above the galactic plane (see Fig. 4 in Young et al., 1988).

trated in a warped disk and a ring of similar dimension (Fig. 10 below). Since NGC 2146 has no companion galaxy (at least when using the criteria of spatial and velocity coincidence; Fisher & Tully 1976), it has been proposed that the starburst is triggered by a far evolved merger (Jackson & Ho 1988, Young et al. 1988, Hutchings et al. 1990, Taramopoulos et al. 2000). However, the meager kinematic and material signature of the merger is far from convincing.

The galaxy is seen nearly edge-on¹ at the inclination $i \approx 60 - 65^\circ$ so that the minor axis is tilted by $\epsilon = 90^\circ - i \approx 25 - 30^\circ$ out of the plane of the sky; the position angle of the major axis is $pa \approx 145^\circ$; the morphology is disturbed and distorted; the center is moderately obscured by $A_V \approx 4 - 7$ mag extinction (Benvenuti et al. 1975, Burbidge et al. 1959, Smith et al. 1995). Compared to M 82, the five times larger distance of NGC 2146 makes (detailed) observations more difficult.

3. Optical observations along the minor axis

In long-slit spectroscopy observations, the position-velocity signature of the outflow is determined by the geometry of the outflow cones (b , Θ , and the skewness of the cones with respect to the galactic plane; see Fig. 9), the velocity of the outflow, the orientation of the galaxy, and the orientation of the slit. Observations with the slit oriented along the minor axis are expected to show velocity-split emission lines, similar to those seen in the outflow of M 82 (McKeith et al. 1995, Shopbell & Bland-Hawthorn 1996). Burbidge et al. (1959) reported line splitting of $\Delta v \approx 300 \text{ km s}^{-1}$ near the center of NGC 2146. Hutchings et al. (1990) mention line splitting, though without further detail. Armus et al. (1995) report that the emission of the outflow is blue-shifted at the NE side and red-shifted at the SW side with a velocity separation of $\sim 130 \text{ km s}^{-1}$, that line splitting of $\Delta v \approx 150 - 200 \text{ km s}^{-1}$ occurs at 1.5 - 3 kpc distance on either side of the galactic plane, and that the line width increases from $\sim 100 \text{ km s}^{-1}$ to 200 - 300 km s^{-1} at a height of ~ 1 kpc. Line splitting was not seen by Benvenuti et al. (1975) and Young et al. (1988).

With the 4.2 m William Herschel telescope (La Palma) we have obtained a spectrogram, containing the $H\alpha$ 6563 Å, [NII] 6548, 6583 Å, and [SII] 6716, 6731 Å emission lines, with the slit oriented along the minor axis ($pa = 50^\circ$) and passing through the eye-estimated 'center' of the galaxy (i.e. the brightest central spot). The velocity resolution determined from sky lines is $\sim 100 \text{ km s}^{-1}$ (FWHM of a Gaussian profile); velocity structures of the line profiles can be determined with a precision of $\sim 30 \text{ km s}^{-1}$. The $H\alpha$ and [NII] 6583 Å line are reproduced in Fig. 1. The picture shows strong line (gas) and continuum (stars) emission in the galactic disk of ~ 0.5 kpc thickness, break-out of the gas from the disk, and faint emission extending into the halo to a height of ~ 3 kpc (limited by the length of the slit and the exposure time of 1800 s). The picture shows noticeable $H\alpha$ emission at a height of ~ 2.5 kpc to the NE. This emission comes from an object in the string of H II regions having a velocity of $\sim +100 \text{ km s}^{-1}$ with respect to the center of the galaxy. This, or a similar H II region, is also seen in the spectrogram taken along the minor axis by Armus et al. (1995, their Fig. 8). The string of H II regions is clearly seen in the pictures published by Young et al. (1988).

4. Outflow velocities

From the $H\alpha$ line (Fig. 1) we have extracted velocity tracings at various heights below and above the galactic plane. These tracings, normalized to the individual peak emission (see also Fig. 4 a below), are shown in Fig. 2 and are interpreted together with Fig. 9 below which explains the proposed geometry of the outflow and the velocity com-

¹ face-on: $i = 0^\circ$.

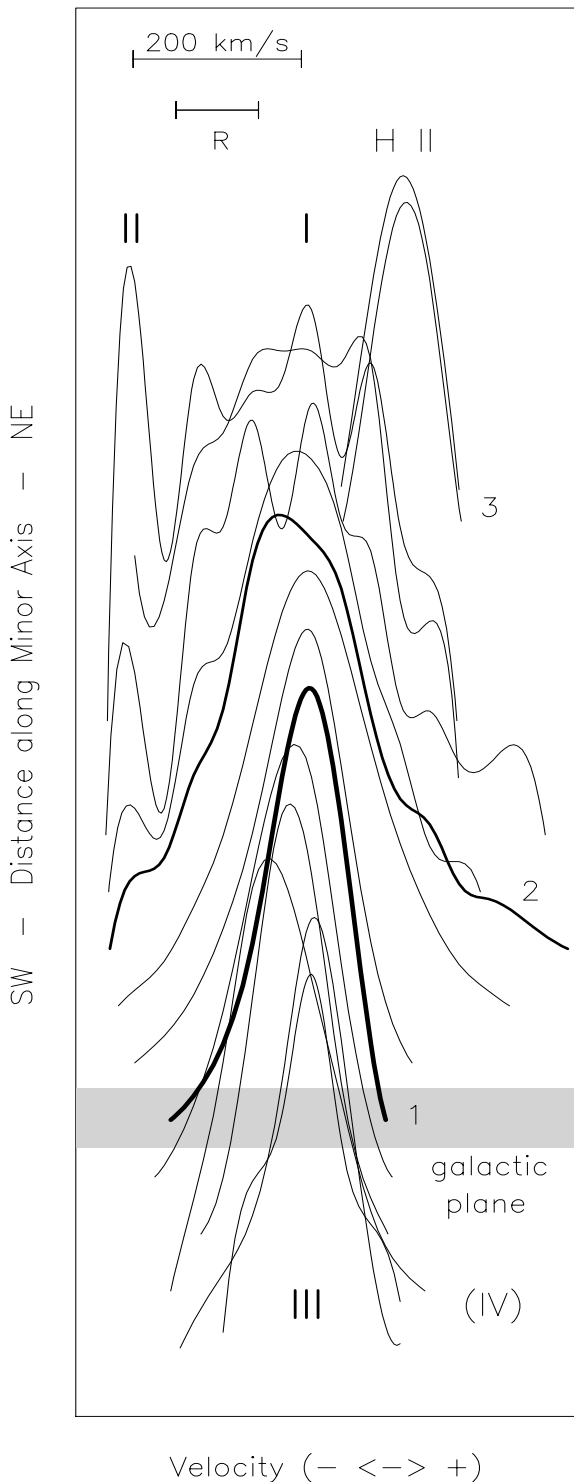


Fig. 2. H_{α} velocity tracings at various heights along the minor axis below (SW) and above (NE) the galactic plane illustrating the differences in profile shape. The components I – (IV) of the outflow cone walls are indicated at their appropriate location along the velocity axis (see also Fig. 9). Profile 1 is extracted at the galactic plane; profile 2 at ~ 0.5 kpc NE above the galactic plane has the largest width; profile 3 is the H II region at the NE (see Fig. 1). The velocity scale and the resolution of the spectrogram (R) is inserted. Intensities are not to scale.

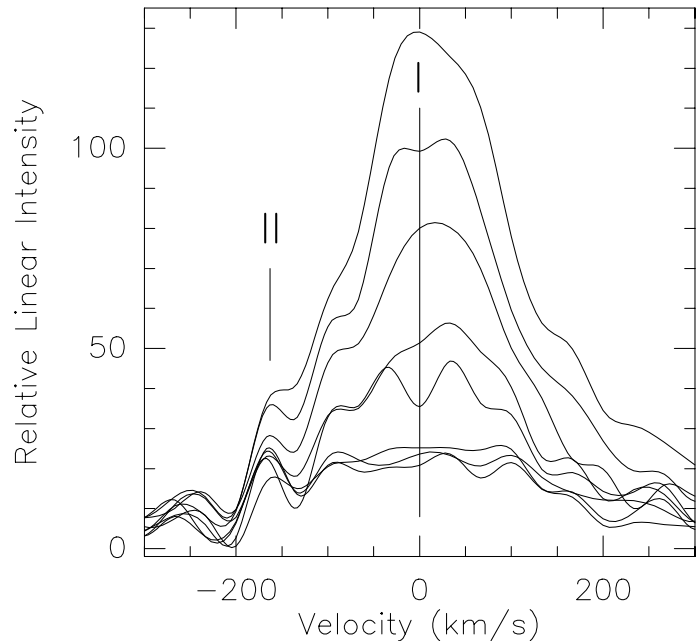


Fig. 3. H_{α} velocity tracings between ~ 0.5 kpc and ~ 1.5 kpc above the galactic plane (NE) where component I and component II are seen. [The noise in the tracings is visible at velocities below -200 km s^{-1} .]

ponents I – IV. Contrary² to the observation by Armus et al. (1995) we do not find a systematic blue/red-shift of the lines at the NE/SW side of the galactic plane (see the straight [NII] line in Fig. 1). Also contrary to their observation, the profiles at the SW side of the galactic plane do not show line splitting, but only component III. The profiles at the NE side show primarily component I, but also some line splitting as illustrated in Fig. 3. The intensity of the tentatively identified component II is *very weak*, however, the appearance of component II in several tracings covering a distance of ~ 1 kpc NE along the minor axis (between ~ 0.5 kpc and ~ 1.5 kpc) gives confidence of its existence. At ~ 1.5 kpc NE above the galactic plane the splitting between component I (at positive velocities) and component II (at negative velocities) is $\Delta v \approx 200 \text{ km s}^{-1}$; a similar value was found by Armus et al. (1995). The width of $300 - 400 \text{ km s}^{-1}$ of profile 2 (Fig. 2) at ~ 0.5 kpc NE above the galactic plane is probably due to acceleration of the outflow when breaking out of the galactic plane, similar as seen in M 82 (McKeith et al. 1995, their Fig. 2). The component IV at the SW is not seen. We interpret the observation that component I and III appear at *nearly* the same and constant velocity (Fig. 2) by the fact that the line-of-sight is *nearly* perpendicular to the corresponding cone walls. For a similar situation in M 82, where all components are observed, see McKeith et al. (1995).

² part of the observed spectral differences are certainly due to different slit positions.

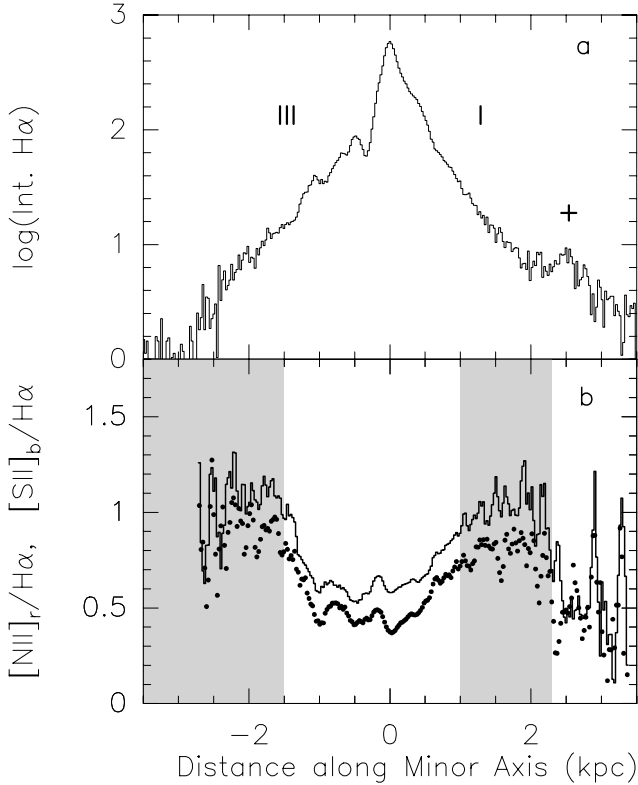


Fig. 4. (a) $H\alpha$ emission (logarithm of relative units) measured along the minor axis. Gas of the minor axis outflow is indicated by the shaded areas. Outside the galactic disk, the intensities at the SW and NE side are primarily emission of component III and component I (see Fig. 2, 3 & 9). The mark (+) indicates the H II region at ~ 2.5 kpc NE above the disk (see Fig. 1). (b) Ratios $[NII]_r/H\alpha$ (line) and $[SII]_b/H\alpha$ (dots) which indicate thermally excited gas (≈ 0.5) and gas with a contribution of shock excited gas (≈ 1). SW is to the left, NE to the right.

5. Line ratios and density

The $[NII] 6583/H\alpha \equiv [NII]_r/H\alpha$ and $[SII] 6716/H\alpha \equiv [SII]_b/H\alpha$ line ratios are used to investigate shock excitation of the ionized gas; the $[SII] 6716/6731$ line ratio is used to derive the electron density n_e (for $T_e = 10^4$ K) (Osterbrock 1989, Lehnert & Heckman 1996 b). These line ratios need no correction for differential extinction, but the location in the galaxy to which they refer depends on the line-of-sight absorption (probably not exceeding $A_V \approx 4-7$ mag at the center). The $H\alpha$ emission, and the $H\alpha$ line profiles extracted in the galactic disk, may need a correction for underlying stellar $H\alpha$ absorption. We have no data of the stellar line, and neglect the influence in the following comparative study.

We have extracted from the spectrogram of Fig. 1 the line ratios $[NII]_r/H\alpha$ and $[SII]_b/H\alpha$ shown in Fig. 4 b. The values of this figure agree with the observations by Armus et al. (1995, their Fig. 6). At the center of the galaxy, and to a height of 0.5 – 1 kpc above the disk, we find values of

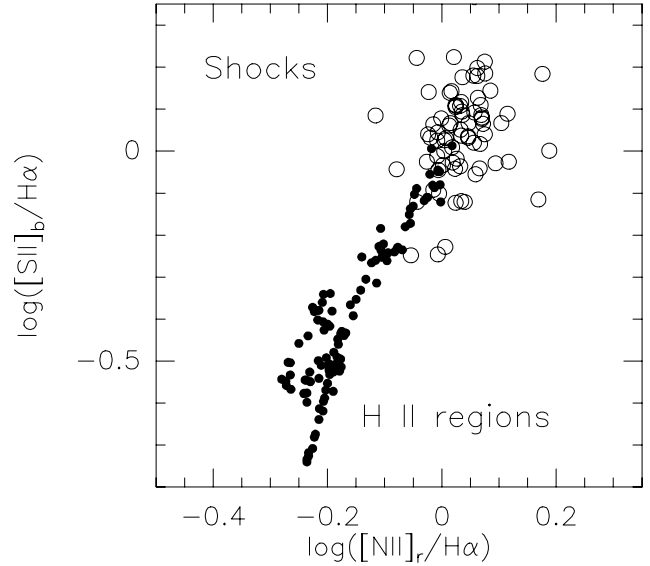


Fig. 5. Line ratio diagram of gas measured along the minor axis. Open circles: outflow gas at a height of -3 kpc $\lesssim z \lesssim -1.5$ kpc and 1 kpc $\lesssim z \lesssim 2.3$ kpc below and above the galactic plane (shaded region in Fig. 4 b) containing a contribution of shock excited gas. Dots: gas at a height of -1.5 kpc $\lesssim z \lesssim 1.2$ kpc containing thermally excited gas, primarily in the galactic disk. For similar diagrams of Diffuse Interstellar Gas in galaxies see Rand (1998) and Lehnert & Heckman (1996 b).

~ 0.5 as typical for thermally excited ionized gas in H II regions. This is confirmed by the clear signature of the H II region gas at ~ 2.5 kpc NE above the disk. Between ~ 1 kpc and ~ 2 kpc above the disk the line ratios gradually increase to ~ 1 and remain at this value to a height of 3 kpc, indicating ionized gas with a noticeable contribution of shock excited gas (Rand 1998, Martin 1998, Wang et al. 1999, Lehnert & Heckman 1996 b, Reynolds et al. 1999), as expected to be present in the walls of the outflow cones³. The additional diagnostic diagram Fig. 5 confirms that the gas at a height of -3 kpc $\lesssim z \lesssim -1.5$ kpc and 1 kpc $\lesssim z \lesssim 2.3$ kpc above the plane, which in essence is gas of the outflow, contains a contribution of shock excited gas, while the gas at lower heights is thermally excited.

The line ratio $[SII] 6716/6731$ (see footnote 3) is 0.90 – 0.95 in the galactic disk, ~ 1.1 at a height of 1.5 – 2 kpc above the plane, and ~ 1.4 (the low density value) at 2.5 – 3 kpc height. These observed values and the corresponding electron densities are given in Table 1. The values seem to indicate a decrease of the electron density in the cone walls with height z which, when approximated by a z^{-2} depen-

³ The line ratios can, in principle, only be calculated for the individual components I – IV (for M82 see McKeith et al. 1995). We explain below (Fig. 9) the geometry of the outflow cones and the reason of using the line ratios of the velocity-integrated emission NE and SW of the disk.

Table 1. Electron density (n_e , for $T = 10^4$ K) of the ionized gas in the Galactic Disk and the Cone Walls of the outflow in NGC 2146.

	Height z [kpc]	[SII]6716/6731 (observed)	n_e [cm^{-3}]
Galactic Disk	0 – 0.5	0.90 – 0.95	~ 600
Cone Walls	1.5	1.1	300
"	2.5	1.4	$\lesssim 100$

dence of the electron density as found for M 82 (McKeith et al. 1995), gives

$$n_e \approx 600 [\text{cm}^{-3}] (z/\text{kpc})^{-2} \quad (1)$$

The values at ~ 1.5 kpc $\lesssim z$ are uncertain and need additional observations.

6. Radio observations

6.1. Plateau de Bure CO interferometer observations

We have used the PdB interferometer in a 7-mosaic observation to map the starburst region in the optically thick ^{12}CO (1–0) line and the optically thin ^{13}CO (1–0) line (for the optical thickness see Xie et al., 1995). For a description of the PdB observations and the results see Greve et al. (in prep.). In these observations, and the ^{12}CO (1–0) observation by Young et al. (1988), we believe that there is evidence of some molecular material which is dragged-out along the minor axis. In other starburst galaxies, for instance M 82, a similar drag-out of molecular material (CO) into the halo was already proposed in 1987 by Nakai et al. (1987); a possible outflow of dust was recently suggested by Thuma et al. (2000). A molecular outflow along the minor axis of NGC 253, though only to a height of ~ 150 pc above the galactic plane, was recently observed by García-Burillo et al. (2000).

6.2. Dragged-out molecular material

The velocity channel maps of the interferometer measurements by Young et al. (1988) and Greve et al. (in prep.) cover the starburst region in ^{12}CO and ^{13}CO and show the bulk of molecular material of the ring and warp and ‘fingers’ of emission which extend more or less skew out of the galactic plane, similar to ‘chimneys’ or ‘galactic fountains’ seen at radio and optical wavelengths. We believe that these outflow features provide evidence of gas and dust being dragged-out of the disk at the inner periphery of the molecular ring by the superwind of the starburst. This material gives information on the geometry of the outflow.

For several selected velocity channels of the ^{12}CO (1–0) and ^{13}CO (1–0) line, observed at PdB, we show in Fig. 6 and Fig. 7 the features which we interpret to indicate outflow. The method of deriving from these measurements

the position and direction of the outflow (with respect to the galactic plane) is illustrated for the ^{12}CO (1–0) channel map at -62 km s $^{-1}$ (Fig. 6). In this figure the dashed line is the galactic plane. The skew solid lines, above and below the galactic plane, indicate at 0.3 – 0.5 kpc height a component of dragged-out molecular material and the direction of the outflow. The base of this outflow is near the intersection of the solid lines with the galactic plane; the relative height of the outflow is the distance of a selected lowest contour measured in the direction of the outflow. We have investigated corresponding channel maps of the ^{12}CO (1–0) (Fig. 6) and the ^{13}CO (1–0) (Fig. 7) line in order to assess that the observed features are not produced by an optical depth effect. The correspondence is good, taking into account the ~ 10 times weaker intensity of the ^{13}CO line. This and similar evidence from other observations is used in Fig. 8 for a determination of the outflow geometry.

7. Derivation of the outflow geometry

In analogy to similar phenomena observed in M 82, we believe that the *ensemble* of several emission features provides also in NGC 2146 evidence of the outflow and information of the outflow geometry:

a) *X-ray emission.* The ROSAT observations show X-ray emission extending out of the galactic plane as a feature called *x-shaped* by Armus et al. (1995, their Fig. 3). A tentative interpretation of the X-ray image is emission confined to a bi-conical outflow of opening angle $\Theta \approx 60 - 70^\circ$, $pa \approx 35^\circ$, and diameter at the base of $b \lesssim 2$ kpc. Armus et al. mention that the X-ray emission is detected up to a height of ~ 4 kpc above the galactic plane.

b) *Synchrotron emission.* Interferometer observations between 327 MHz and 15 GHz by Lisenfeld et al. (1996) show essentially a bar-like distribution of the emission, but also extensions skew and perpendicular out of the galactic plane, resembling galactic chimneys or galactic fountains. Fig. 8 a shows the position and position angles of these extensions seen at 8.4 GHz in the observations by Lisenfeld et al. Similar chimneys were recently detected in M 82 by Wills et al. (1999).

c) *Dust ‘fingers’.* The optical images published by Young et al. (1988) and Hutchings et al. (1990) show several prominent dust ‘fingers’ extending skew to the SE away from the galactic plane. This dust may consist of cool material being dragged-out of the disk by the superwind of the starburst, rather than being only material of spiral arm III (de Vaucouleurs 1950, Benvenuti et al. 1975). The position and position angles of the dust ‘fingers’ are shown in Fig. 8 a.

d) *Dragged-out molecular gas.* We believe, as explained above, that the velocity channel maps of the ^{12}CO and ^{13}CO lines (Young et al. 1988, their Fig. 2; Fig. 6 & 7) indicate molecular gas being dragged out of the disk by the superwind of the starburst. From these observations we

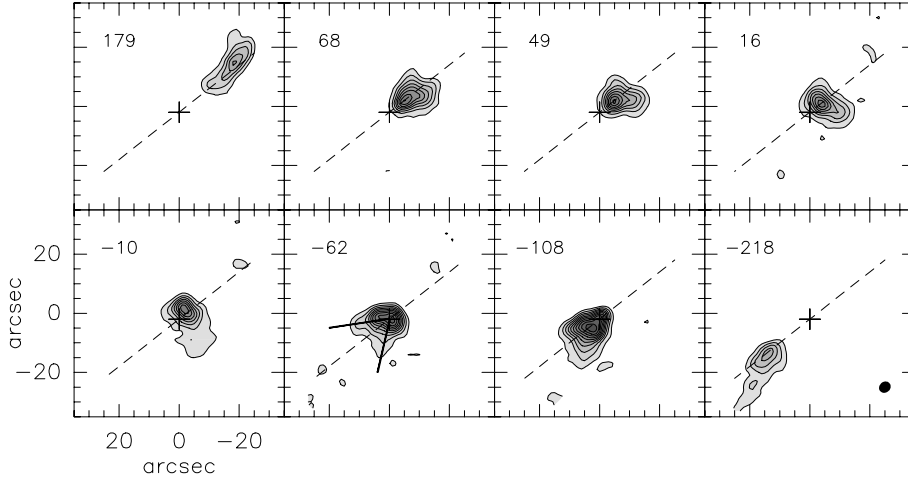


Fig. 6. Selected velocity channel maps (with the systemic velocity of 850 km s^{-1} subtracted) showing **12** CO (1–0) material assumed to be dragged-out of the galactic plane. The method of deriving the position and direction of the outflow is illustrated for the channel map at -62 km s^{-1} . The dashed line is the galactic plane; the solid lines indicate the direction of the outflow. The solid dot in the lower box is the synthesized beam of $4.1'' \times 3.6''$ [$290 \text{ pc} \times 250 \text{ pc}$]. Contour levels from 0.05 to 0.8 Jy/beam, by 0.075. The coordinates are centered (cross) at $6^{\text{h}} 18^{\text{m}} 38.6^{\text{s}}$, $78^{\circ} 21' 24.0''$ (2000). N is up, E is left.

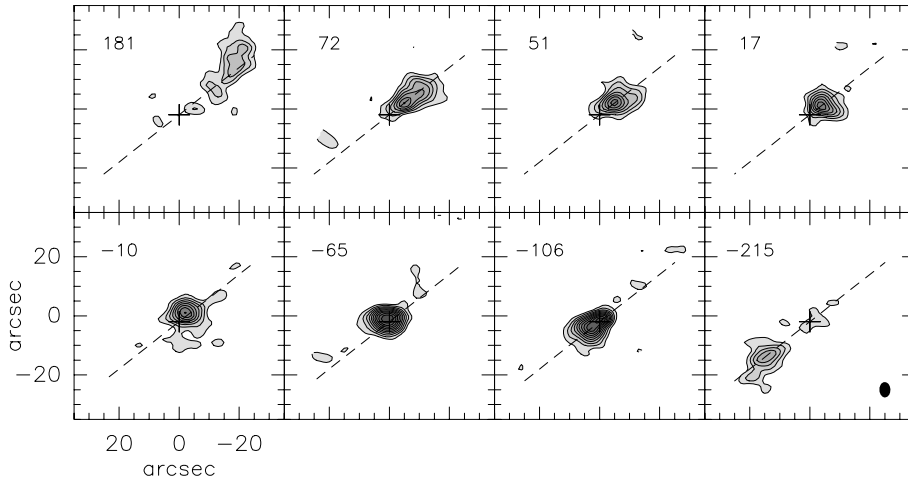


Fig. 7. Same as Fig. 6, but for the approximately *ten times weaker* **13** CO (1–0) line. Contour levels from 0.005 to 0.1 Jy/beam, by 0.005. The synthesized beam is $5.2'' \times 3.6''$ [$360 \text{ pc} \times 250 \text{ pc}$].

extracted the positions and position angles of the dragged-out molecular gas as shown in Fig. 8 b & 8 c.

NGC 2146 rotates anti-clockwise, i.e. from SE to NW. It is expected that the outflow material carries part of this rotation, hence angular momentum, out of the disk into the halo. To illustrate this effect (Fig. 8 c) we note that the dragged-out material which is oriented away from the galactic disk in the direction North and West is seen at similar positive velocities as the rotation of the NW part of the galaxy ($r \leq 0$); the dragged-out material which is oriented in the direction East and South is seen at similar negative velocities as the rotation of the SE part of the galaxy ($0 \leq r$). In the direction toward the center of the starburst the dragged-out material is seen at small veloci-

ties and oriented nearly perpendicular out of the galactic disk.

8. The outflow

We explain the features of Fig. 1, 2, 3 & 8 as a bi-conical outflow along the minor axis with opening angle $\Theta \approx 60^\circ$ and diameter at the base of $b = 1.0 - 1.5 \text{ kpc}$, i.e. the same as the distance between the emission peaks of the CO ring (Table 2 below). The outflowing material is collimated by the material of the molecular ring. The geometry of this outflow⁴ is schematically shown in Fig. 9. In order to agree with the observed velocities of component I and II, in this

⁴ for a similar figure of M 82 see McKeith et al. (1995).

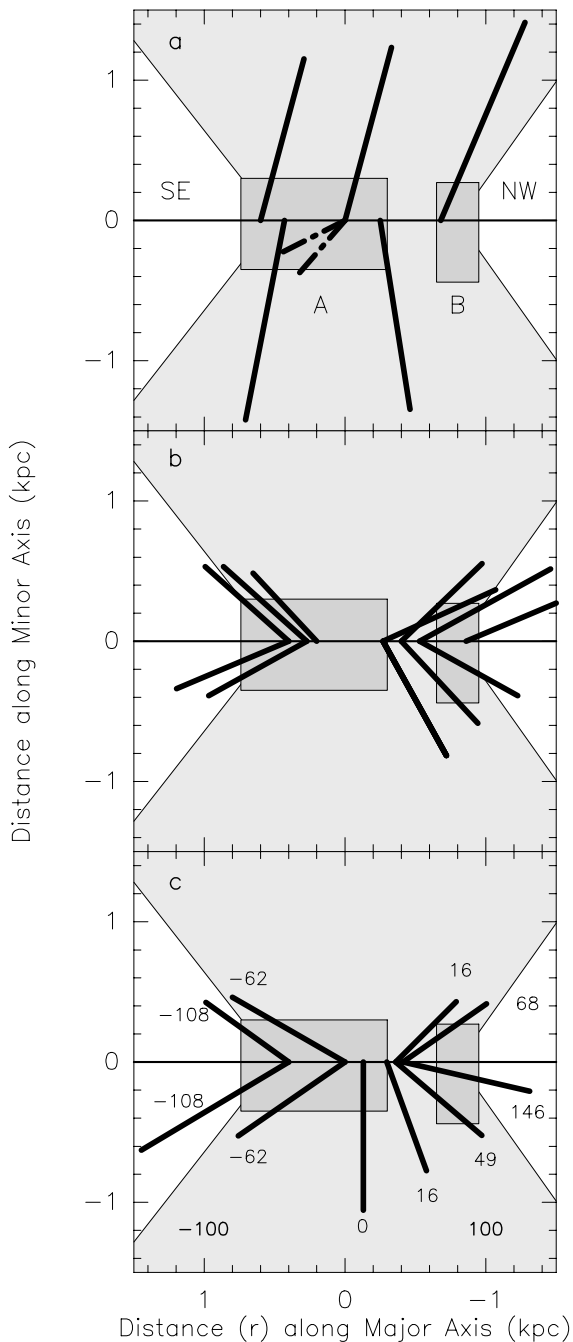


Fig. 8. Derivation of the outflow base (b) and cone opening angle (Θ). The horizontal line is the galactic plane; the rectangular boxes show schematically the Eastern (A) and Western (B) emission peaks of the CO ring (Fig. 10). The shaded area shows the adopted idealized outflow cone and its intersection with the galactic plane. The skew lines show ‘outstreamers, fingers, chimneys’ of (a) 8.4 GHz continuum emission (Lisenfeld et al. 1996): heavy lines; dust fingers (Young et al. 1988, Hutchings et al. 1990): dashed lines; (b) ^{12}CO (1–0) (Young et al. 1988); (c) ^{12}CO (1–0) (this paper). The rotation of the galaxy is $\pm 100 \text{ km s}^{-1}$ at $\pm 1 \text{ kpc}$ radial distance. The numbers in the plot indicate the velocity (km s^{-1}) at which the outflows are detected (see also Fig. 6).

interpretation the NE part of the galaxy is necessarily tilted toward us. Since the minor axis tilt $\epsilon = 90^\circ - i$ and the half opening angle of the cone ($\theta = \Theta/2$) are *nearly* the same, i.e. $\epsilon \approx \theta \approx 25 - 30^\circ$, the rear side (I) of the NE cone and the front side (III) of the SW cone are seen *nearly* perpendicular to the line-of-sight so that the corresponding observed outflow velocity components are small, or zero. These outflow components I and III are seen in the spectrogram Fig. 1. The front side (II) of the NE cone and the rear side (IV) of the SW cone are inclined by $\epsilon + \theta \approx 60^\circ$ to the line-of-sight. For $\epsilon = \theta = 30^\circ$ and a particular line-of-sight, the distances along the cone walls are

$$r_a = r(\text{I}) = r(\text{III}) = (z - d) \cos(\epsilon), \quad (b/2) \tan(\epsilon) \leq z \quad (2)$$

$$r_b = r(\text{II}) = r(\text{IV}) = [r_a + b \sin(\epsilon)] / \cos(\epsilon + \theta) \quad (3)$$

with z the vertical height above the galactic plane and d the semi-thickness of the galactic disk (0.3 – 0.5 kpc). Using the density relation $n_e(z)$ of Eq.(1), the fact that the emission is proportional to n_e^2 , and the assumption that the cone walls have a (constant) thickness L , the intensity \mathcal{I} of the emission is

$$\mathcal{I}_{a,b} \propto (n_{e,a,b})^2 L \propto (r_{a,b})^{-4} L \quad (4)$$

The observed decrease of the $\text{H}\alpha$ emission along the components I and III (i.e. \mathcal{I}_a) shown in Fig. 4 a agrees reasonably well with this prediction. Since $r_b(\text{II,IV}) \approx 3 r_a(\text{I,III})$, we have $\mathcal{I}_b(\text{II,IV}) \approx (1/100) \mathcal{I}_a(\text{I,III})$. This unfavourable intensity ratio explains why the components II and IV are not (easily) seen in a spectrogram taken along the minor axis (Fig. 1). For this reason, in addition, we have calculated line ratios along the minor axis without taking into account possible line splitting (Fig. 4 & 5).

The observed velocity difference between component I and component II at a height of 1 – 2 kpc NE above the galactic plane is $\Delta v \approx 200 \text{ km s}^{-1}$, with component II located at the blue side of component I (Fig. 2 & 3) in agreement with the geometry of Fig. 9. A similar value Δv is reported by Armus et al. (1995), however also for the SW side of the galactic plane. Since component I appears at a small velocity, we interpret $\Delta v \approx V^*$ as the blue-shifted line-of-sight velocity component of the outflow velocity V along cone wall II. From the geometry of the outflow we then obtain $V = V^* / \sin(\epsilon + \theta) \approx 250 - 300 \text{ km s}^{-1}$. This velocity is small compared to the terminal velocity of $\sim 600 \text{ km s}^{-1}$ predicted from the model by Chevalier & Clegg (1985), and compared to the outflow velocity of $500 - 600 \text{ km s}^{-1}$ measured in M82 (Table 2). This fact may contradict the tentative identification of component II. However, adopting a very different geometry to avoid this situation would be in conflict with the data of Fig. 8. An explanation of this relatively low outflow velocity may be found in the much larger starburst volume of NGC 2146, as compared to M82, the lower material density in the starburst region, and in the apparently three

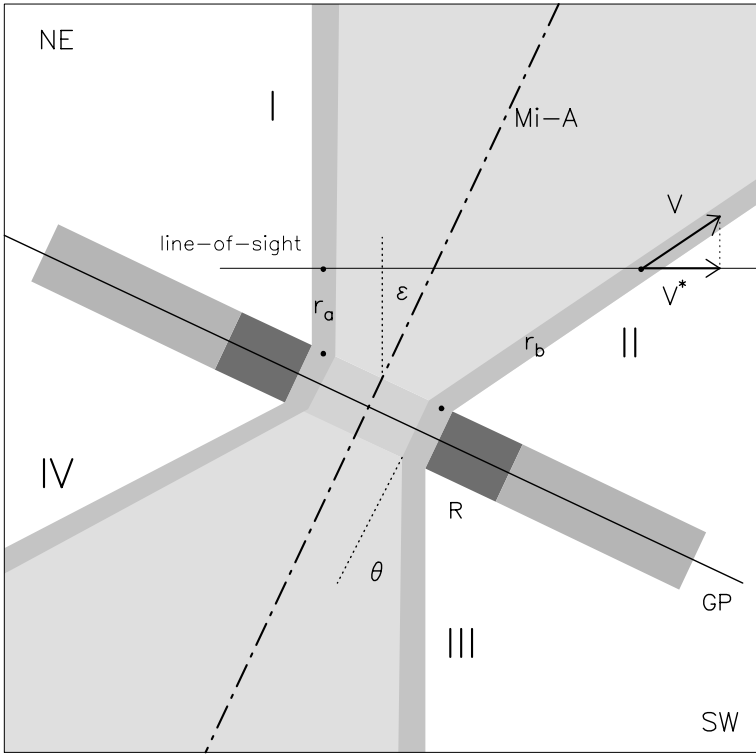


Fig. 9. Illustration of the outflow geometry of NGC 2146. GP is the galactic plane, R the CO ring, Mi-A the minor axis, the observer is at the right side. The tilt of the minor axis is $\epsilon = 90^\circ - i$ with $i = 60 - 65^\circ$ the inclination of the galaxy. θ is the half opening angle of the cones, i.e. $\epsilon \approx \theta \approx 30^\circ$. The outflow cones, filled with X-ray emitting gas, and the cone walls I – IV, emitting optical recombination lines, are shown. r_a and r_b are the distances along the cone walls from the galactic disk to the respective intersections with the line-of-sight. V is the outflow velocity, V^* the line-of-sight component. The diameter of the galactic disk, as shown here, is ~ 6 kpc.

times *smaller* number of observed radio supernovae and supernova remnants in NGC 2146 (Tarchi et al. 2000), although the estimated star formation rate (Table 2 below), and hence supernova rate, seems to be three times higher. The larger volume, lower density, and the proportionally smaller number of radio supernovae and supernova remnants may produce in NGC 2146 an outflow which is less funneled because of the larger base and larger opening angle, and which is hence more diffuse and less propulsive.

The conclusions reached above are based on an idealization of the outflow, which in reality may also be significantly distorted like the morphology of the galaxy. The present collection of observations, which contains some contradictions, does not allow a more precise determination of the actual situation.

Figure 10 shows an overlay of the velocity-integrated $^{12}\text{CO}(1-0)$ emission measured at PdB (Greve et al., in prep.) and the sources detected at 1.6 GHz and 5 GHz (some) with MERLIN and the VLA (Tarchi et al. 2000). The sources are either radio supernovae, supernova remnants, ultra-compact/ultra-dense H II regions which contain massive star clusters or super star clusters. The objects are confined to the region in and inside the CO ring, as expected from their origin in the starburst. This concentration to the CO ring and the inside provides additional evidence that supernova explosions and stellar winds are the primary source of the minor axis outflow. A similar figure for M 82, based on PdB $^{13}\text{CO}(1-0)$ observations and

supernova observations, was published by Neininger et al. (1998, their Fig. 3).

We believe that the ensemble of observations gives a consistent picture of an outflow and of dragged-out material, confined to a region of ~ 2 kpc diameter. Certainly, other explanations can be tested which consider other known structures in and near the starburst region, in particular a clumpy dusty spiral arm viewed under oblique angle and giving the impression of dragged-out material. The dusty ‘spiral arm III’, proposed by de Vaucouleurs (1950), is probably a dust lane(s) with little mass since no trace is seen in deep dust continuum measurements (at 230 GHz), and is located at the edge of the starburst region as indicated by the visual obscuration. The dust lanes are affected by the outflow, as we propose, but hardly affect the outflow. The incomplete string of H II regions, giving the impression of a spiral arm, is in fact an inclined $\sim 10 \times 20$ kpc ellipsoidal pattern partially projected onto the center region of the galaxy. This string of H II regions does not affect the outflow and is not affected by the outflow (Greve et al. in prep.). The 700 pc long, triple-source S-shaped pattern seen by Kronberg & Biermann (1981) at the center of NGC 2146 has been resolved into more sources hardly giving the impression of a mini-spiral arm (Tarchi et al. 2000). On the other hand, the CO velocity pattern, in particular measured in the region $\sim \pm 800$ pc \times 250 pc along the major axis (i.e. inside the 3rd contour in Fig. 10), is that of a regularly rotating disk

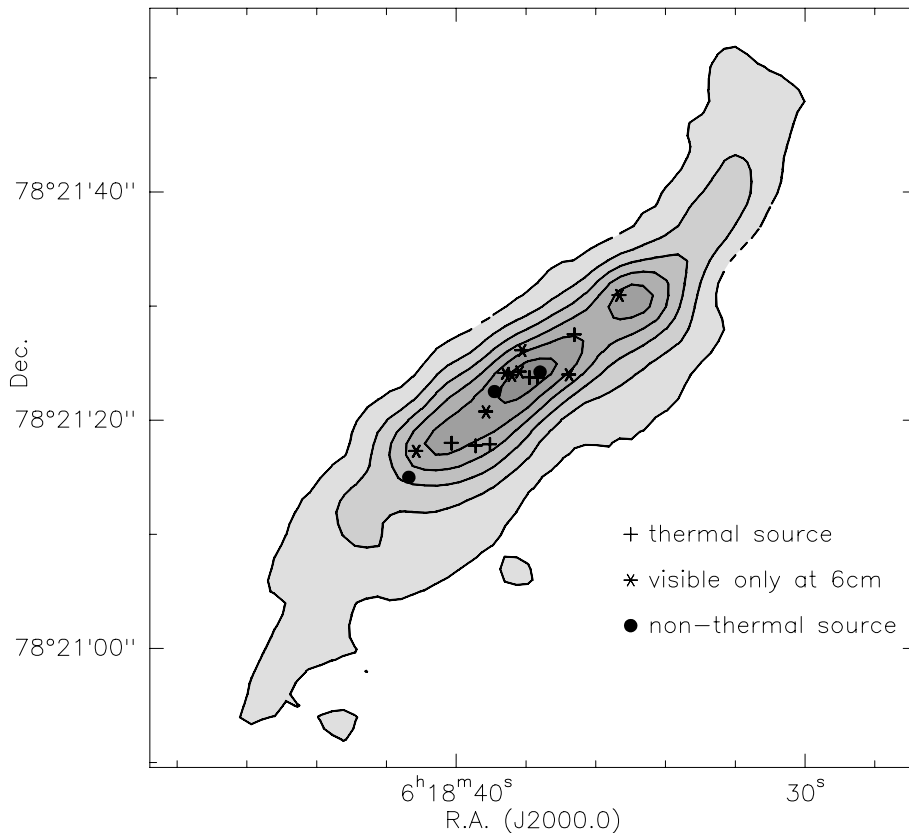


Fig. 10. Velocity-integrated ^{12}CO (1-0) emission (Greve et al., in prep.) and radio sources observed with MERLIN and the VLA (Tarchi et al. 2000).

and ring without perturbations. Above ~ 300 pc on either side of the galactic plane the velocity distribution flares out into the halo in a regular bi-cone like pattern (Greve et al., in prep.). The regularity of this velocity pattern in and above the galactic plane makes it difficult to envisage an alternative distribution of material and motions inside ~ 2 kpc diameter, which produces similar features as shown in Fig. 8, than that of a starburst region with outflow.

Table 2 compares the dimension of the starburst and the outflow in NGC 2146 with the prototype starburst and outflow in M 82. The significantly larger geometric scale and activity of the starburst phenomenon in NGC 2146 is evident.

9. Summary

Using a combination of radio, optical, and X-ray observations, we have tried to derive the geometry and physical state of an *idealized* minor axis outflow in NGC 2146: the outflow is conical on either side of the galactic plane; the diameter at the base is $b \approx 1000$ pc, comparable in diameter with the molecular ring; the opening angle is $\Theta \approx 60^\circ$; near the base the hot outflowing material drags gas and dust out of the disk; the outflowing material carries angular momentum into the halo; the cone walls of the outflow can be traced (at optical wavelengths) to a height of $h \approx 3$ kpc; the (electron) density in the cone walls seems

to decrease proportional to z^{-2} , with z the height above the galactic plane; the outflow velocity at ~ 1 kpc height is $250 - 300 \text{ km s}^{-1}$.

While these parameters of the outflow give a consistent explanation of the radio, optical, and X-ray observations, the absence of velocity component IV and the low outflow velocity along the cone walls (at least cone wall II) may speak against the proposed interpretation. However, compared with M 82, the larger dimension of the starburst region and of the molecular ring, and an apparently smaller number of radio supernovae and supernova remnants seem to produce a larger flaring of the outflow (b , Θ), and by this possibly a less propulsive outflow with a lower velocity. The weak component IV may also partially be hidden by the galactic disk, but its absence may also be in line with the general distortion of the galaxy. The coincidence of ultra-compact/ultra-dense H II regions, radio supernovae, and supernova remnants with the region of the CO ring and the interior gives confidence in the picture of a superwind driven minor axis outflow.

Acknowledgements. We are thankful for the optical observations which were made in service time with the William Herschel Telescope (WHT) operated on the Island of La Palma by the INT Group in the Spanish Observatorio de Roque de los Muchachos of the Instituto de Astrofísica de Canarias. M. Bremer (IRAM) helped with the production of Figure 1. We

Table 2. Minor Axis Outflows of NGC 2146 and M 82.

Parameter	NGC 2146 ^{a)}	M 82 ^{a,b)}
Distance	14.5 Mpc	3.2 Mpc
The Starburst Region		
Diameter starburst region	2 500 pc	850 pc
Volume starburst region	2×10^{10} pc ³	3×10^8 pc ³
Diameter molecular ring (inside)	750 pc	550 pc
Radial thickness molecular ring (Δr)	1000/600 pc ^{c)}	250 pc
Thickness molecular ring (Δz)	500 pc	150 pc
Mass of starburst region	$\sim 1 \times 10^{10} M_{\odot}$	$\sim 2 \times 10^9 M_{\odot}$
Density starburst region	$\sim 1/4 M_{\odot} \text{pc}^{-3}$	$\sim 3 M_{\odot} \text{pc}^{-3}$
Infrared luminosity (L_{FIR}) ^{d)}	$7.0 \times 10^{10} L_{\odot}$	$2.4 \times 10^{10} L_{\odot}$
Star formation rate (SFR) ^{e)}	5 – 15 $M_{\odot} \text{yr}^{-1}$	2 – 6 $M_{\odot} \text{yr}^{-1}$
The Outflow		
Inclination galaxy (i) ^{f)}	$\sim 60^{\circ}$	$\sim 80^{\circ}$
Visibility cones	I, (II), III, –	I, II, III, IV
Outflow base (b)	1 000 pc	500 pc
Cone opening angle ($\Theta = 2\theta$)	60°	25°
Outflow height (h)	~ 4 kpc	2 kpc (10 kpc) ^{g)}
Volume of cones (up to $h \approx 3$ kpc)	5×10^{10} pc ³	1×10^{10} pc ³
Outflow velocity (at $h \approx 1$ kpc)	250 – 300 km s^{-1}	500 – 600 km s^{-1}
Outflow acceleration	–	100 – 150 $\text{km s}^{-1} \text{kpc}^{-1}$
Cone wall density (at $h \approx 1$ kpc)	$\sim 300 \text{cm}^{-3}$	$\lesssim 100 \text{cm}^{-3}$

a) Greve et al., in prep.

b) Shopbell & Bland–Hawthorn (1998), southern cone; McKeith et al. (1995).

c) Eastern/Western section (see Fig. 8 & 10).

d) $L_{\text{FIR}} = 6 \times 10^5 D^2 [\text{Mpc}] (2.58 F_{60} [\text{Jy}] + F_{100} [\text{Jy}])$ (Thronson & Telesco 1986).

e) a best estimate from several authors using different methods.

f) face-on: $i = 0^{\circ}$.

g) Devine & Bally (1999).

thank the referee for his comments and we agree with his remark that the presented picture is a tentative interpretation of the sometimes scarce evidence of the outflow phenomenon.

References

- Armus L., Heckman T.M., Weaver K.A., Lehnert M.D. 1995, ApJ 445, 666
- Axon D.J., Taylor K. 1978, Nature 274, 37
- Benvenuti P., Capaccioli M., D’Odorico S. 1975, A&A 41, 91
- Bland J., Tully R.B. 1988, Nature 334, 43
- Bregman J.N., Schulman E., Tomisaka K. 1995, ApJ 439, 155
- Burbidge E.M., Burbidge G.R., Prendergast K.H. 1959, ApJ 130, 739
- Chevalier R.A., Clegg A.W. 1985, Nature 317, 44
- Della Ceca R., Griffiths R.E., Heckman T.M., Lehnert M.D., Weaver K.A. 1999, ApJ 514, 772
- de Vaucouleurs G. 1950, Ann. Astrophys. 13, 362
- Devine D., Bally J. 1999, ApJ 510, 197
- Fisher J.R., Tully R.B. 1976, A&A 53, 397
- García–Burillo S., Martín–Pintado J., Fuente A., Neri S. 2000, A&A 355, 499
- Heckman T.M., Armus L., Miley G.K. 1990, ApJS 74, 833
- Hutchings J.B., Lo E., Neff S.G., Stanford S.A., Unger S.W. 1990, AL 100, 60
- Jackson J.M., Ho P.T.P. 1988, ApJ 324, L 5
- Kronberg P.P., Biermann P. 1981, ApJ 243, 89
- Lehnert M.D., Heckman T.M. 1996 a, ApJ 462, 651
- Lehnert M.D., Heckman T.M. 1996 b, ApJ 472, 546
- Lisenfeld U., Alexander P., Pooley G.G., Wilding T. 1996, MNRAS 281, 301
- Martin C.L. 1997, ApJ 401, 561
- McKeith C.D., Greve A., Downes D., Prada F. 1995, A&A 293, 703
- Muxlow T.W.B., Pedlar A., Wilkinson P.N. 1994, MNRAS 266, 455
- Nakai N., Hayashi M., Handa T., Sofue Y., Hasegawa T. 1987, PASJ 39, 685
- Neininger N., Guelin M., Klein U., García–Burillo S., Wielebinski R. 1998, A&A 339, 737
- Osterbrock D.E. 1989, *Astrophysics of Gaseous Nebulae and Active Galactic Nuclei*, University Science Books, Mill Valley, CA, USA
- Rand R.J. 1998, ApJ 501, 137
- Reynolds R.J., Haffner L.M., Tuft S.L. 1999, ApJ 525, L 21
- Schaaf R., Pietsch W., Biermann P.L., Kronberg P.P., Schmutzler T. 1989, ApJ 336, 722
- Shopbell P.L., Bland–Hawthorn J. 1998, ApJ 493, 129
- Smith B.J., Harvey P.M., Lester D.F. 1995, ApJ 442, 610
- Taramopoulos A., Payne H., Briggs F.H. 2000, A&A (submitted) (astro-ph/0005370)
- Tarchi A., Neininger N., Greve A., Klein U., Garrington S.T., Muxlow T.W.B., Pedlar A., Glendenning B.E. 2000, A&A 358, 95

- Thuma G., Neininger N., Klein U., Wielebinski R. 2000, *A&A* 358, 65
- Thronson H.A., Telesco C.M. 1986, *ApJ* 311, 98
- Tomisaka K., Ikeuchi S. 1988, *ApJ* 330, 695
- Umemura S., Iki K., Shibata K., Sofue Y. 1988, *PASJ* 40, 25
- Wang J., Heckman T.M., Lehnert M.D. 1997, *ApJ* 491, 114
- Wills K.A., Redman M.P., Muxlow T.W.B., Pedlar A. 1999, *MNRAS* 309, 395
- Xie S., Young J., Scoerb F.P. 1994, *ApJ* 421, 434
- Yokoo T., Fukue J., Taniguchi Y. 1993, *PASJ* 45, 687
- Young J.S., Claussen M.J., Kleinmann S.G., Rubin V., Scoville N. 1988, *ApJ* 331, L 81